UNSTEADY PRESSURE MEASUREMENTS ON A SUPERCRITICAL AIRFOIL AT HIGH REYNOLDS NUMBERS

R. W. HESS
UNSTEADY AERODYNAMICS BRANCH
NASA LANGLEY RESEARCH CENTER

MODEL AND TEST CONDITIONS

The supercritical airfoil on which the measurement was made, Sc(2)-0714, was developed at Langley (Ref. 1), was fourteen percent thick, and had a six-inch chord and an eight inch span. The model was machined from Vascomax-200 which has superior dimensional stability properties at cryogenic temperatures. The tests were conducted in the Langley 0.3 Meter Transonic Cryogenic Tunnel (Ref. 2), .3-m TCT, at Reynolds numbers, R, which varied from 6×10^6 to 35×10^6 at Mach numbers between 0.65 and 0.74. The higher Reynolds numbers were near the edge of the tunnel operating boundary which has a stagnation temperature of 120° Kelvin (-243°F) and a stagnation pressure 6.5 atm (Ref. 2). This tunnel was used in the Advanced Technology Airfoil Test (Ref. 3) program in extensive steady flow airfoil studies that demonstrated the necessity for high Reynolds number testing.

EXTERNAL VIEW OF MODEL

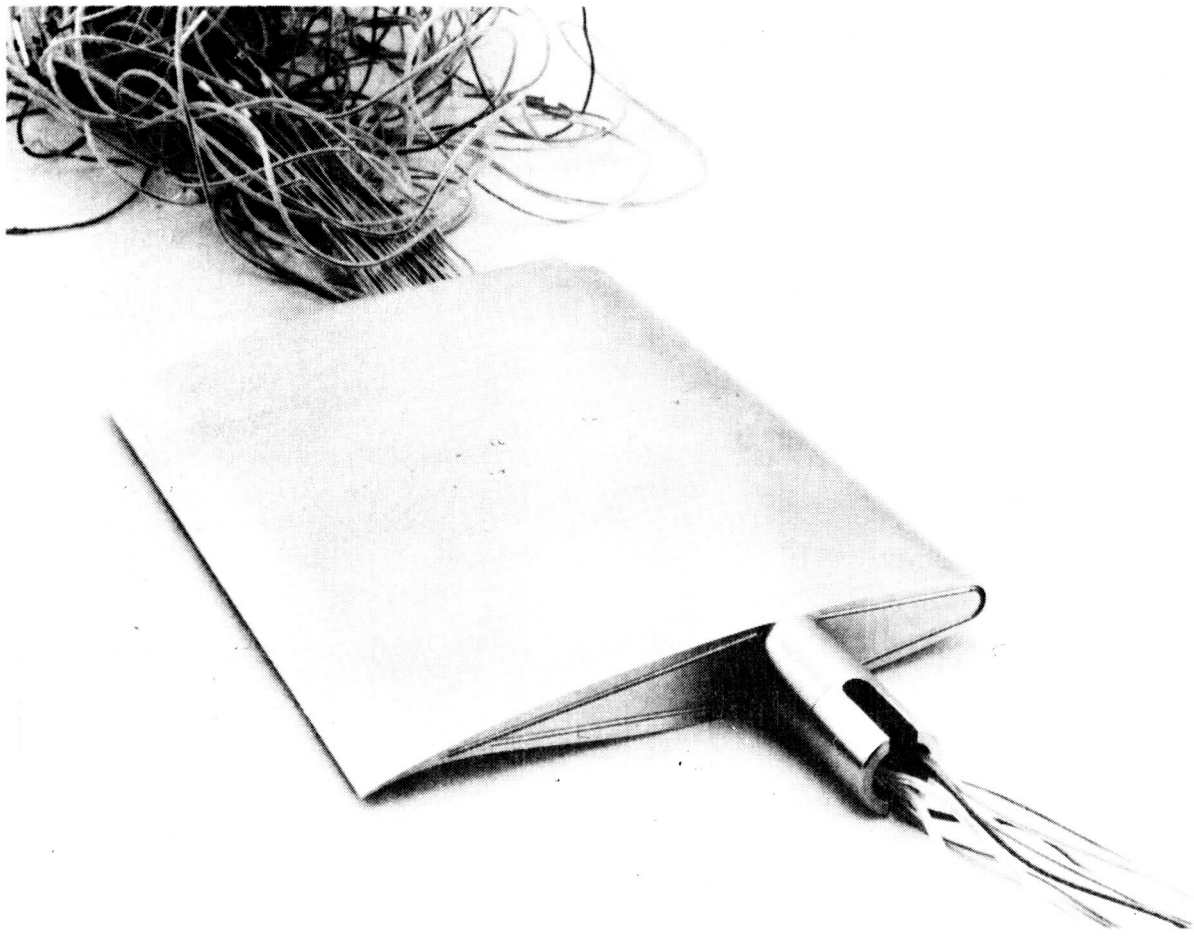

ORIGINAL PAGE
BLACK AND WHITE PHOTOGRAPH

MODEL CONFIGURATION

A cavity machined in the underside of the airfoil provided the space necessary to mount the transducers. The cavity was closed by a cover plate on which some lower surface transducers were mounted. The wing was supported on one end by a close-fitting tang fixed to a driving plate with machine screws; this end, on the left of the figure, was sealed with epoxy . The other end was supported by an integral shaft which rotated in a bushing in the tunnel side wall plate. A sliding seal of felt was used to seal the gap between the end of the oscillating airfoil and the fixed tunnel sidewall plate. The position of the supports was designed to locate the pitch axis at thirty-five percent chord.

INTERNAL CONFIGURATION OF MODEL

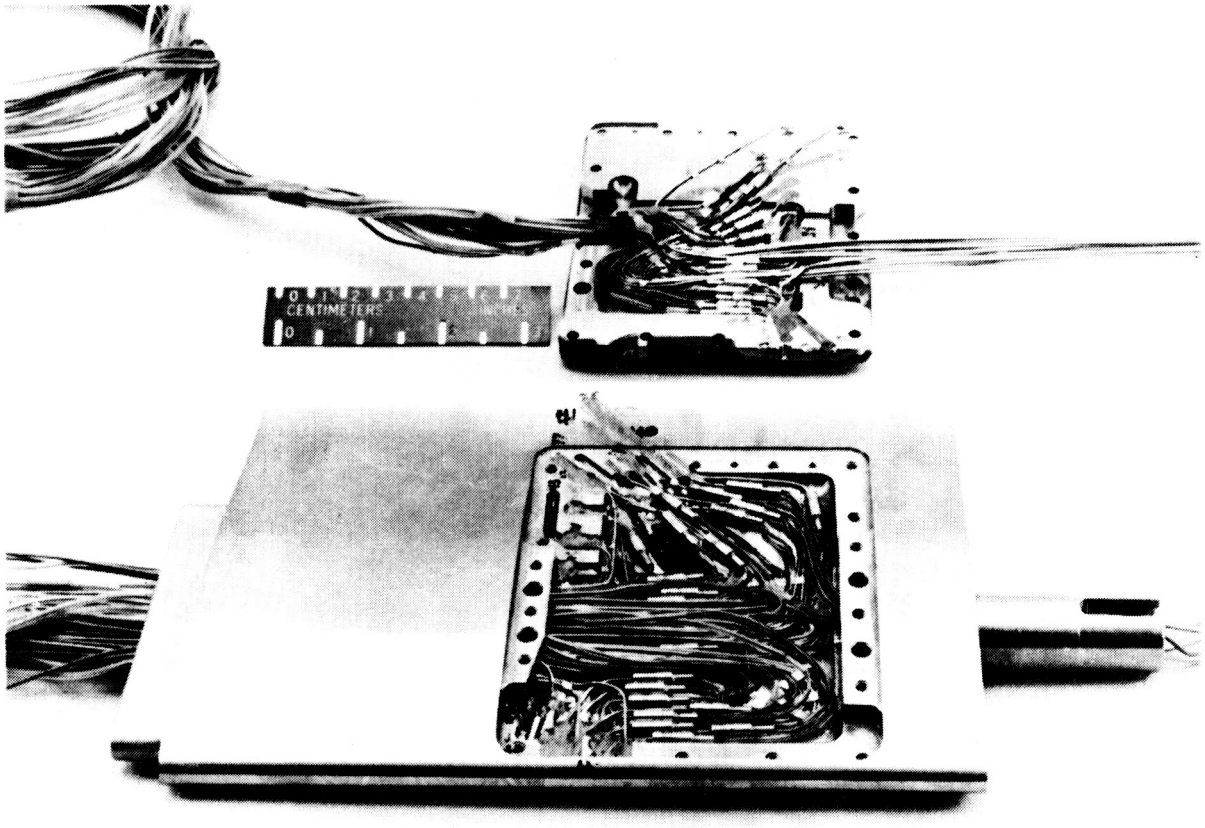

ORIGINAL PAGE
BLACK AND WHITE PHOTOGRAPH

TRANSDUCER LOCATIONS
(TOP SURFACE)

Forty-three unsteady pressure transducers were mounted internally in the model. Forty of the transducers were mounted in receptacles connected to the orifice by a short length of tubing. The remaining three transducers, close mounted, were mounted with the transducer head less than 0.1 inch below the surface of the wing. The distribution of the twenty-seven upper surface transducers is shown in the figure. The receptacle mounted transducer orifices were aligned alternately in two rows 0.25 inches on either side of the airfoil center line. The close mounted transducers orifices and reference orifices were located 0.5 inches from the center line. The orifices of the close-mounted transducers were paired with receptacle-mounted transducer orifices for comparison purposes. The orifices were distributed every 2% chord to x/c of 0.1 and 4% chord to x/c of 0.7.

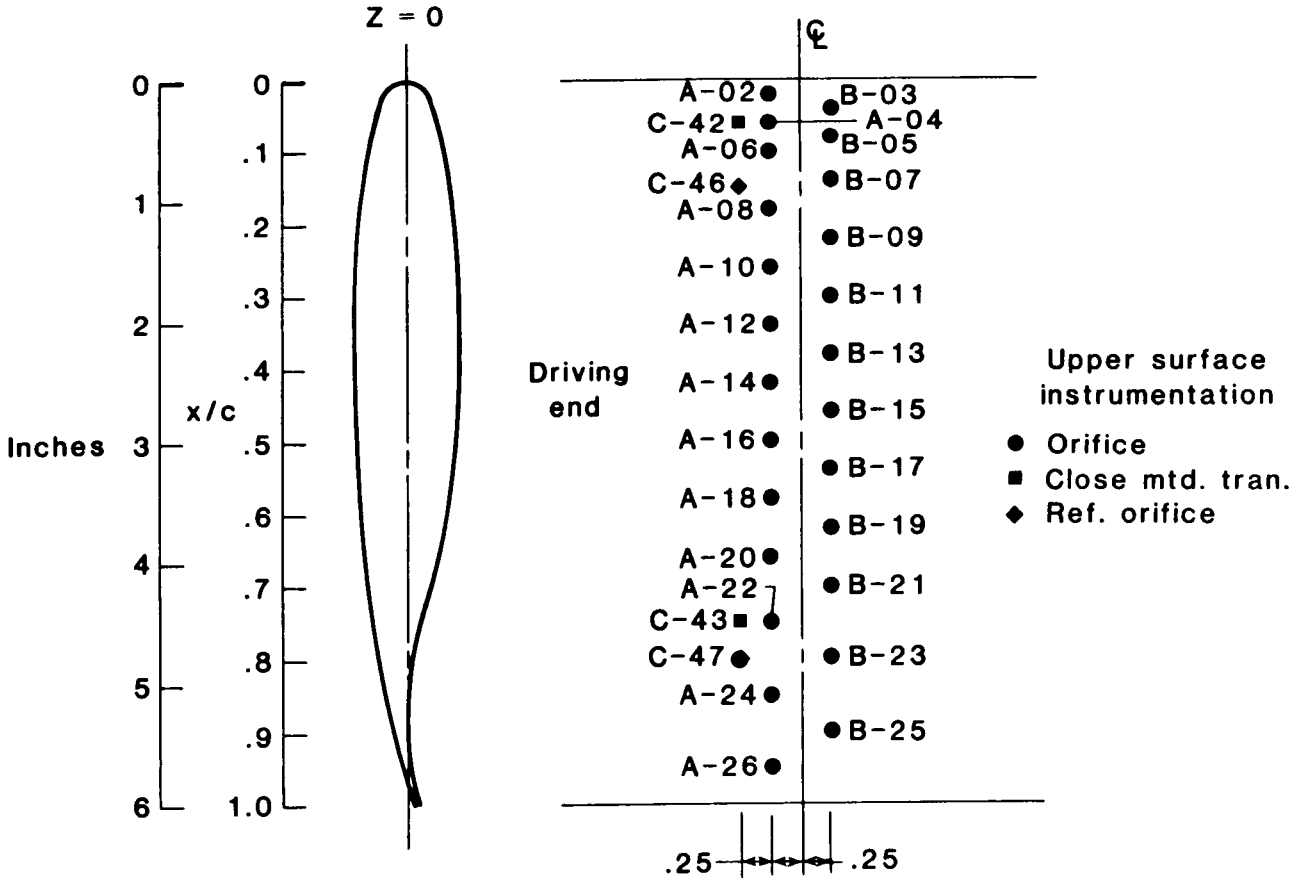

TRANSDUCER LOCATIONS
(BOTTOM SURFACE)

This figure shows the distribution of the 16 transducer orifices on the lower surface; the orifice at the leading edge measured only static pressure. The distribution of the 15 receptacle mounted transducers is more sparse than on the upper surface and is concentrated in regions of largest pressure gradient and is 2% to an x/c of 0.1 and 0.5 thereafter.

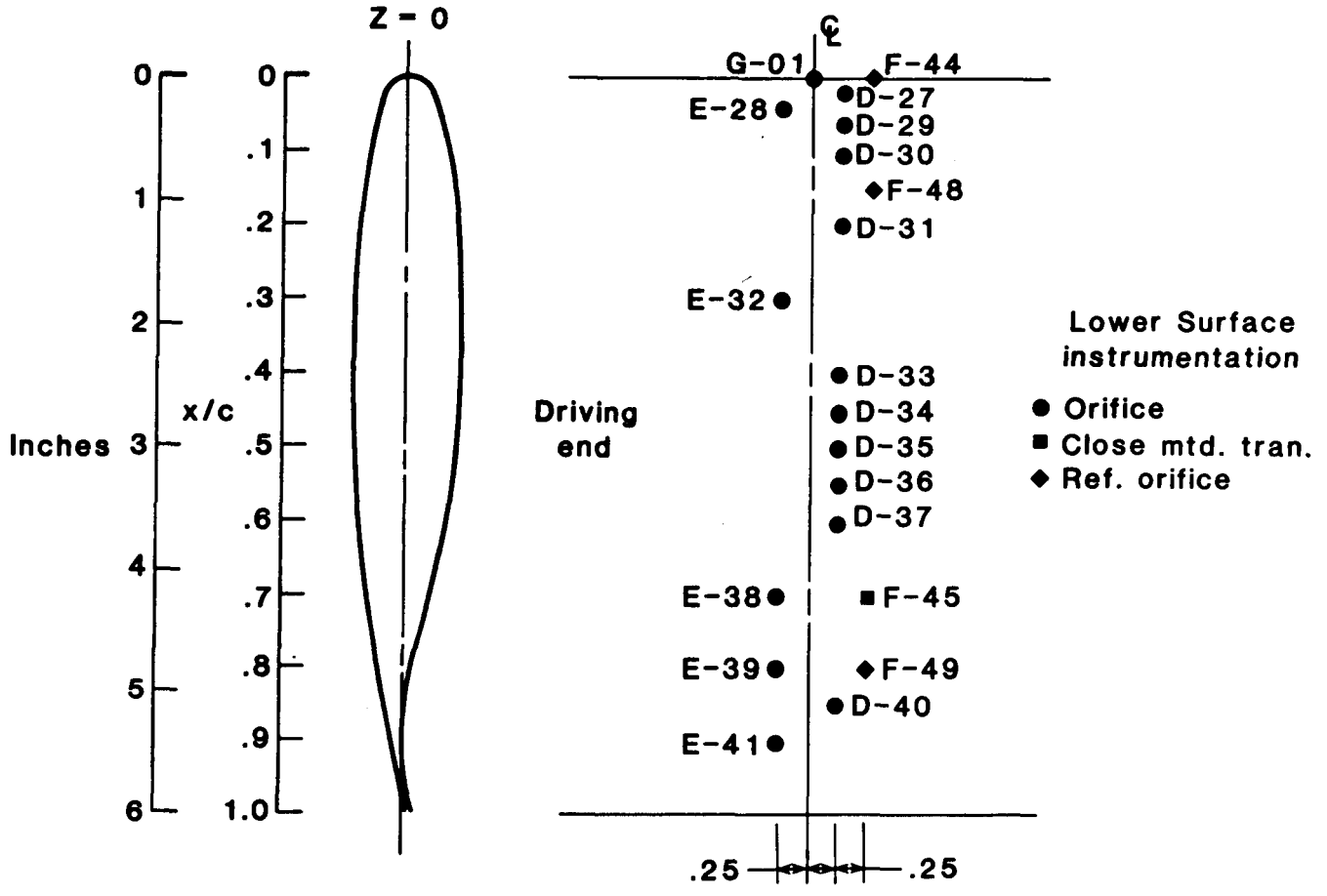

ELEMENTS OF THE TRANSDUCER SYSTEM

The system consisted of transducers, designed for cryogenic application, with a 10 psi range and with outputs of between 5 and 9 mv/psi. Each transducer was mounted in a receptacle which in turn was connected to the 0.015 inch diameter orifice by a 0.75 inch length of 0.030 inch i.d. tubing. Each transducer was referenced to a manifold which in turn was vented to one of five static reference orifices. A reference transducer measured the pressure differential between the manifold and the tunnel static pressure. The connection between the manifold and the reference orifice was interrupted by a porous flow restrictor which damped out the oscillating pressure from the reference orifice. A series of tests were conducted before the model was fabricated to examine the effects of orifice diameter, tube diameter and tube length on the dynamic response of the system. At atmospheric conditions there was no significant reduction of dynamic amplitude response or phase shift of the test configuration up to 100 Hz.

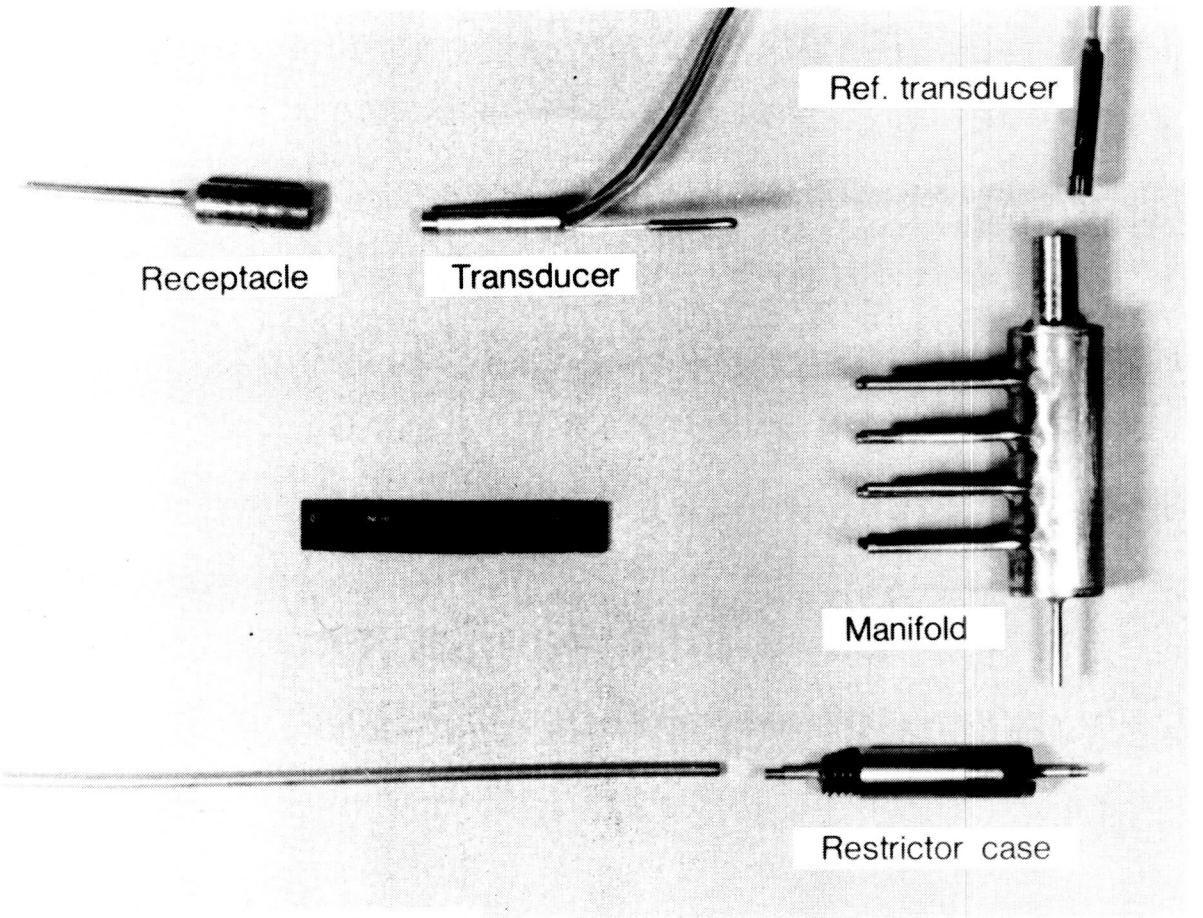

ORIGINAL PAGE
BLACK AND WHITE PHOTOGRAPH

MODEL INSTALLATION

The large variations in temperature (120° k to 320° K) and stagnation pressure (1.4 atm. to 6 atm.) over the operating range of the 0.3-m TCT results in plenum wall deformations that required special consideration in the design of the oscillating drive system. The photograph of the test section, with the ceiling removed, shows the installation of the airfoil and drive system. The hydraulic-rotary actuator required the maintenance of precise alignment during the test. Since the test section floats on a cable suspension system to accommodate thermal contraction, the actuator and supporting structure were also supported by a system of cables and counterweights to enable them to move with the plenum wall.

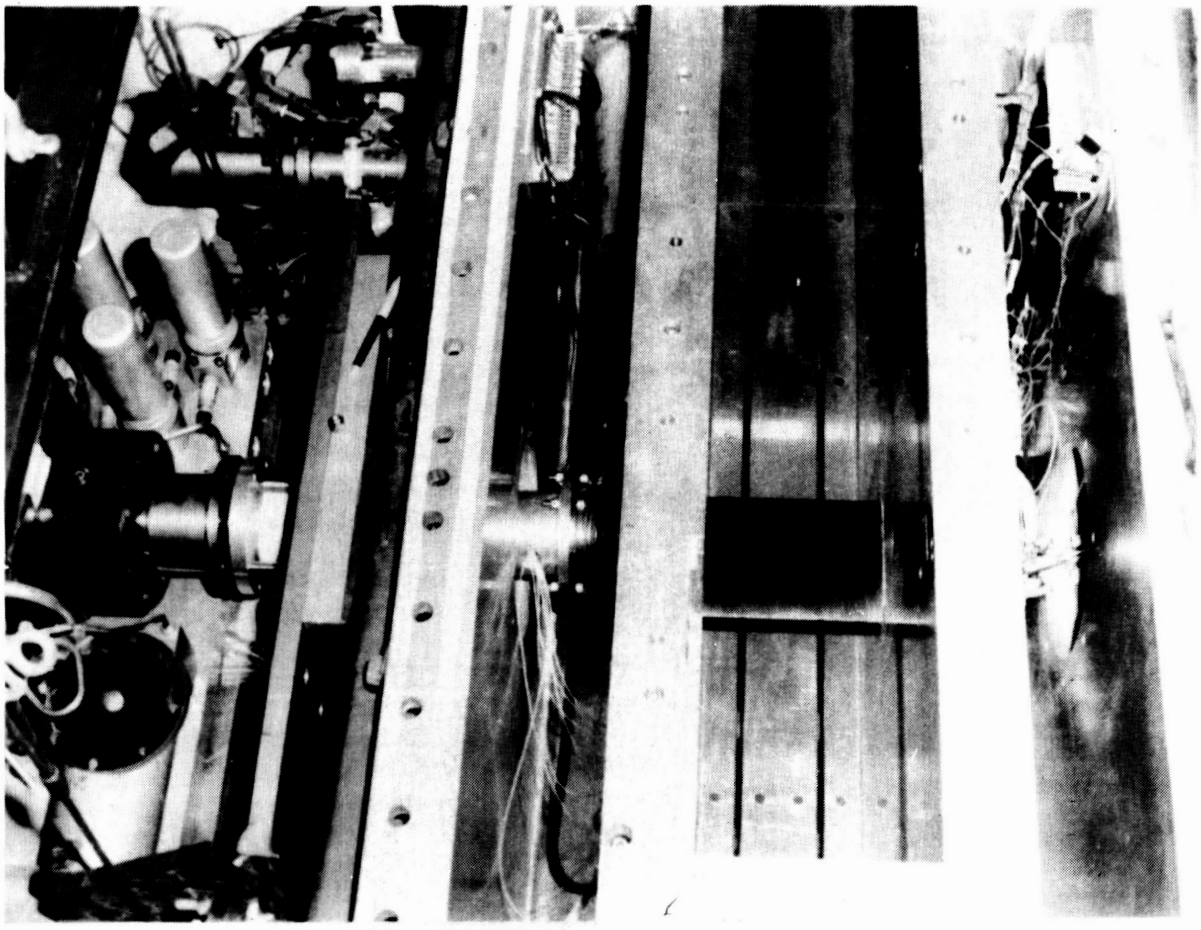

SCHEMATIC OF MODEL INSTALLATION

The critical elements of the oscillating system are identified in this figure. The hollow aluminum drive shaft had fixed point supports at the rotary shaft and at a Teflon bushing and a pressure seal located on the tunnel plenum wall plate. The shaft was attached to the rotating sidewall wall drive disk through a bellows that allowed in-line shaft movement with the plenum wall. The rotating drive disk was Teflon coated on its circumferential bearing surfaces and had a slot to accommodate the wing tang. The tang was hollow to provide a path for transducer cable and tubing. The other edge of the wing was supported by an integral hollow shaft and a bushing in the sidewall plate. The hollow shaft allowed a path for the remaining transducer cables. The rotary transducer, attached to the shaft, was heated with surface heaters under thermostat control and the assembly was covered by an insulating can.

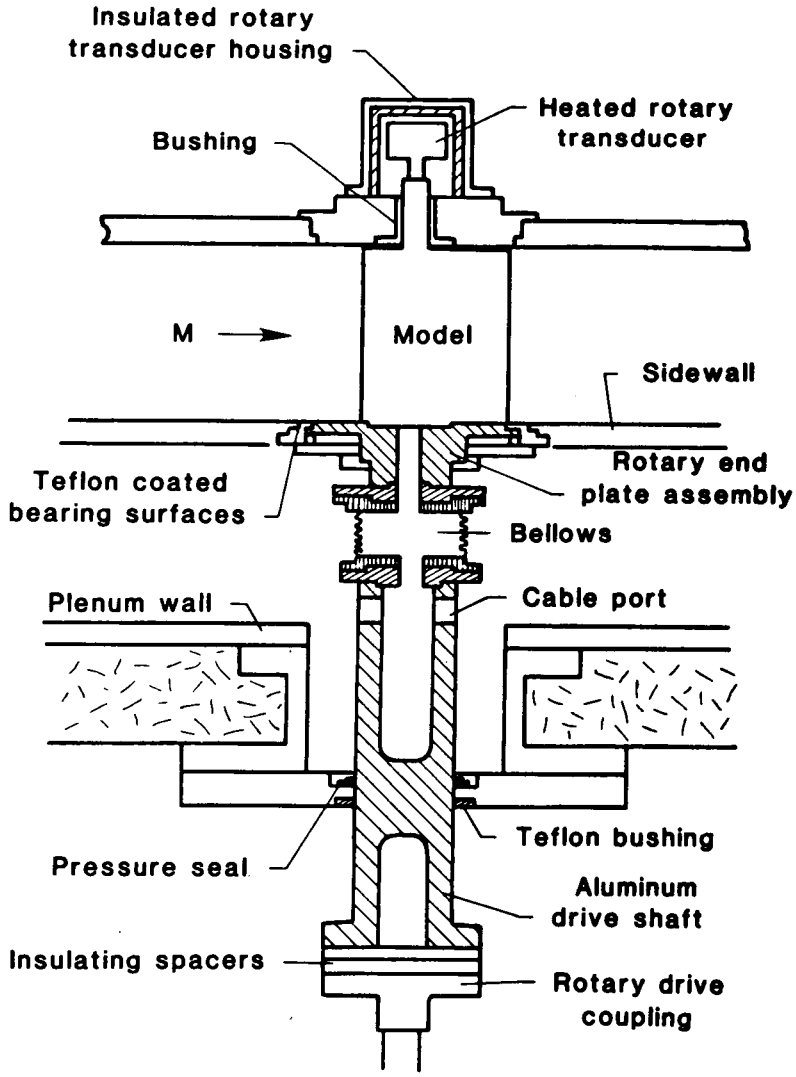

DATA ACQUISITION AND REDUCTION

Steady Pressures - The airfoil and tunnel instrumentation signals were fed to the tunnel data acquisition system through a 10 Hz low-pass filter, digitized at 20 samples/sec and averaged over a one second interval.

Unsteady Pressures - The signals from the amplifiers were recorded on two 28 channel recorders operating at 15 inches per second. This analog data was then digitized at 32 samples/cyc of oscillatory motion for 64 cycles and the harmonic components of the unsteady pressure were determined from FFT analysis. These components were normalized by the harmonic pitch amplitude in degrees. All phase angles were relative to wing position.

Tunnel Corrections - Sidewall boundary-layer and angle of attack corrections were applied to the measured steady pressure results. The sidewall boundary-layer corrections are based on the analysis of Ref. 4 which is used in Ref. 5 with measured values of sidewall displacement and momentum thickness to compile the tables which were used to correct the experimental values in this paper. The angle of attack corrections described in Ref. 6 (sometimes referred to as the "Barnwell-Davis-Moore" correction) adjust the analysis of Davis-Moore with experimental data. The wall induced downwash over the airfoil in the 0.3-m TCT for $C_l = 1.0$ is:

$$\bar{\delta\alpha} = 1.73245^{\circ}$$

MACH NUMBER AND REYNOLDS NUMBER TEST CONDITIONS

The test was designed to explore the effects of Reynolds number on unsteady pressures and to generate a data base for validating unsteady-aerodynamic computer codes. The test conditions as defined by Mach number and Reynolds number are shown in the figure. Test points were taken at the design Mach number of 0.72, determined from data of a previous test, at test Reynolds numbers varying from 6×10^6 to 35×10^6. A total of 976 test points were taken. The primary data base was taken for pitch-oscillation frequency between 5 Hz and 40 Hz at an amplitude of $\pm 0.25^o$ as indicated by the open and solid symbols. Once this data was in hand, the pitch amplitude was increased to $\pm 0.5^o$ and $\pm 1.0^o$ and the pitch frequency increased to 60 Hz at test conditions indicated by the solid symbols.

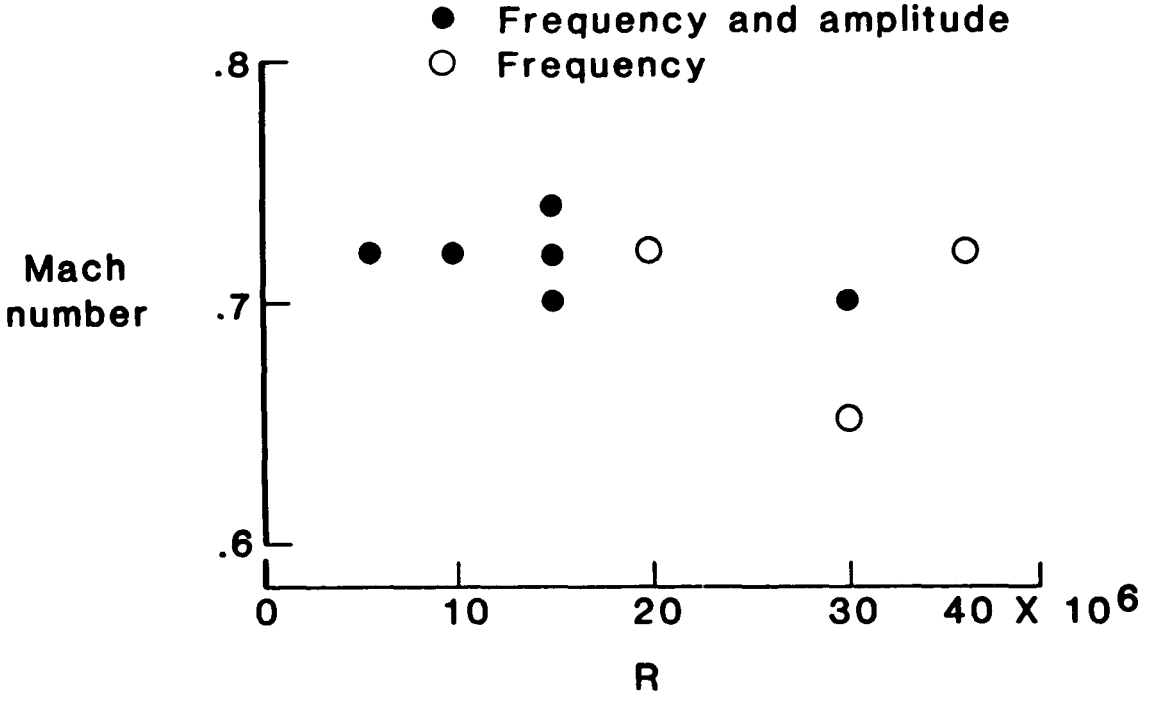

COMPARISONS OF STEADY TEST RESULTS WITH CALCULATED RESULTS AT A TUNNEL MACH NUMBER OF 0.72

$\bar{\alpha}_t \approx 2.5$ degrees

The next four figures give the steady pressure distributions for four angles of attack at two Reynolds numbers, 6 x 10^6 and 30 x 10^6. Experimental data, shown as symbols, are compared with calculated results from GRUMFOIL computer code (Ref. 7) which are shown as solid lines. The GRUMFOIL code consists of a full-potential equation flow solver integrated with a viscous boundary layer model and may be entered by specifying either $\bar{\alpha}$ or C_l. The corrected values of Mach and C_l were used as the input data for the computed results. Below each figure are listed M, $\bar{\alpha}$, and C_l for the tunnel test conditions, the corrected values, and the values resulting from the GRUMFOIL calculations.

$\bar{\alpha}_t \approx 2.5$ deg

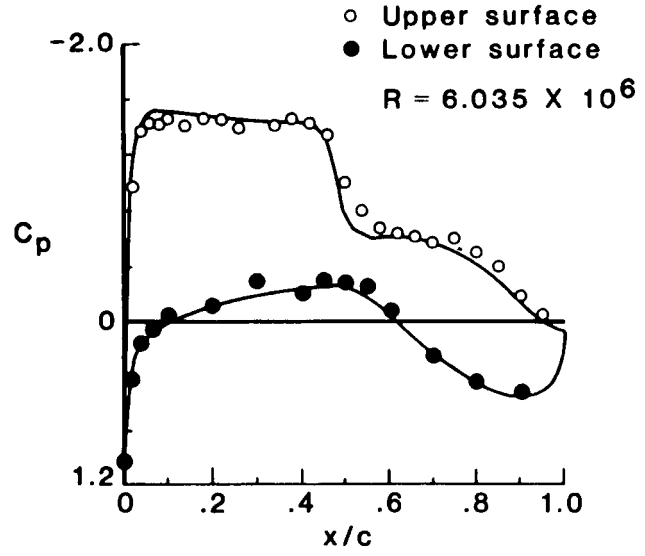

	Tunnel	Corrected	Grumfoil
M	0.720	0.701	0.701
$\bar{\alpha}$	2.504	0.844	1.385
C_l	0.9581	0.9753	0.9837

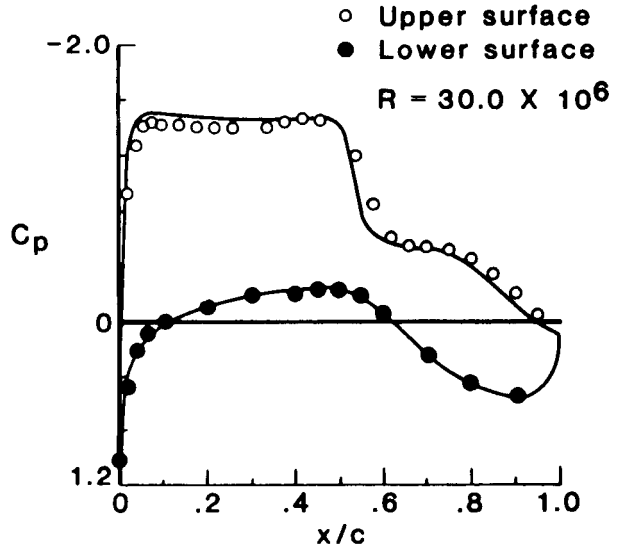

	Tunnel	Corrected	Grumfoil
M	0.719	0.705	0.705
$\bar{\alpha}$	2.51	0.756	1.399
C_l	1.0123	1.0256	1.0336

COMPARISONS OF STEADY TEST RESULTS WITH CALCULATED RESULTS AT A TUNNEL MACH NUMBER OF 0.72

$\bar{\alpha}_t \approx 2.0$ degrees

The comparisons between the experiment, shown as symbols, and GRUMFOIL calculations, solid lines, are very good. The shock moves aft by approximately 8% to 10% of chord for a given value of tunnel mean angle of attack, $\bar{\alpha}_t$, when Reynolds number is increased from 6 x 10^6 to 30 x 10^6. The code under-predicts the position of the shock at both Reynolds numbers by approximately 2-3% of chord even through C_l is matched.

COMPARISONS OF STEADY TEST RESULTS WITH CALCULATED RESULTS AT A TUNNEL MACH NUMBER OF 0.72

$\bar{\alpha}_t \approx 2.0$ deg

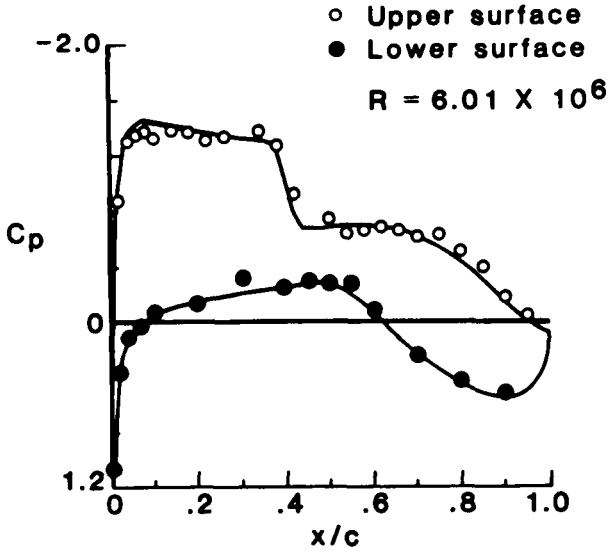

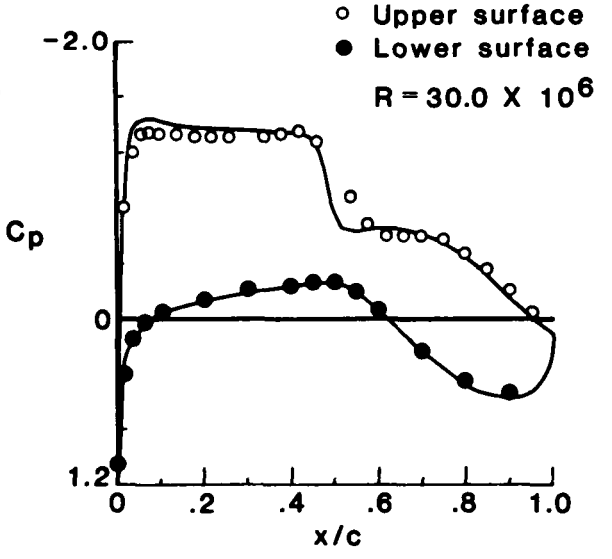

	Tunnel	Corrected	Grumfoil
M	0.72	0.701	0.701
$\bar{\alpha}$	2.002	0.525	0.961
C_l	0.8523	0.8676	0.8757

	Tunnel	Corrected	Grumfoil
M	0.721	0.705	0.705
$\bar{\alpha}$	1.997	0.393	0.910
C_l	0.926	0.939	0.9453

COMPARISONS OF STEADY TEST RESULTS WITH CALCULATED RESULTS AT A TUNNEL MACH NUMBER OF 0.72

$\alpha_t \approx 1.5$ deg

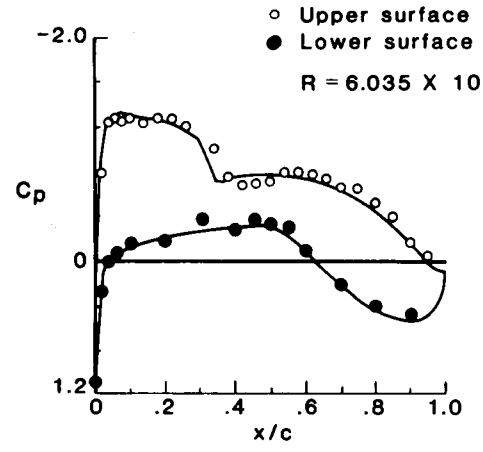

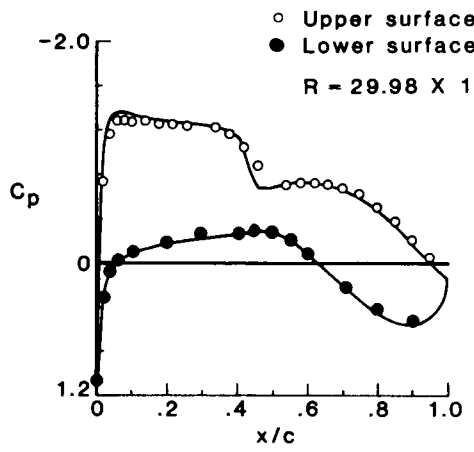

	Tunnel	Corrected	Grumfoil
M	0.719	0.701	0.701
$\bar{\alpha}$	1.495	0.201	0.493
C_l	0.7467	0.7601	0.7680

	Tunnel	Corrected	Grumfoil
M	0.718	0.705	0.705
$\bar{\alpha}$	1.501	0.051	0.552
C_l	.8373	0.849	0.8555

COMPARISONS OF STEADY TEST RESULTS WITH CALCULATED RESULTS AT A TUNNEL MACH NUMBER OF 0.72

$\bar{\alpha}_t \approx 0.0$ deg

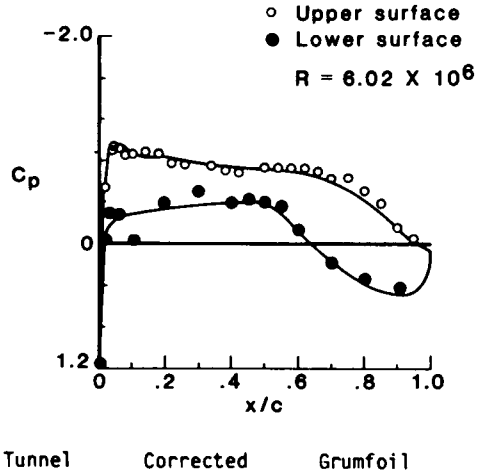

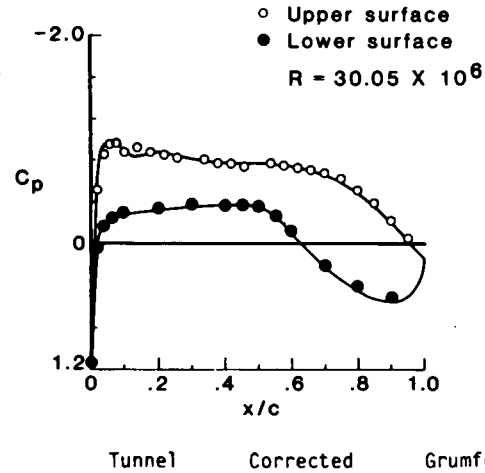

	Tunnel	Corrected	Grumfoil
M	0.720	0.701	0.701
$\bar{\alpha}$	0.004	-0.92	-0.398
C_l	0.5288	0.5383	0.5484

	Tunnel	Corrected	Grumfoil
M	.721	0.705	0.705
$\bar{\alpha}$	-0.005	-1.036	-0.715
C_l	0.5951	0.6034	0.6099

COMPARISON OF LIFT COEFFICIENT VERSUS CORRECTED ANGLE OF ATTACK

Lift coefficients for several cases are shown in this figure plotted against corrected angle of attack and against angle of attack as computed by GRUMFOIL code for input values of Mach number and C_l for Reynolds numbers of 6 x 10^6 and 30 x 10^6. The angles calculated by the code are consistently larger than those determined by the correction procedure of Ref. 6. Irrespective of angle of attack corrections, an increase in C_l of approximately 0.1 is shown as Reynolds number is increased from 6 x 10^6 to 30 x 10^6. This increase results from the rearward movement of the shock shown in the previous figures.

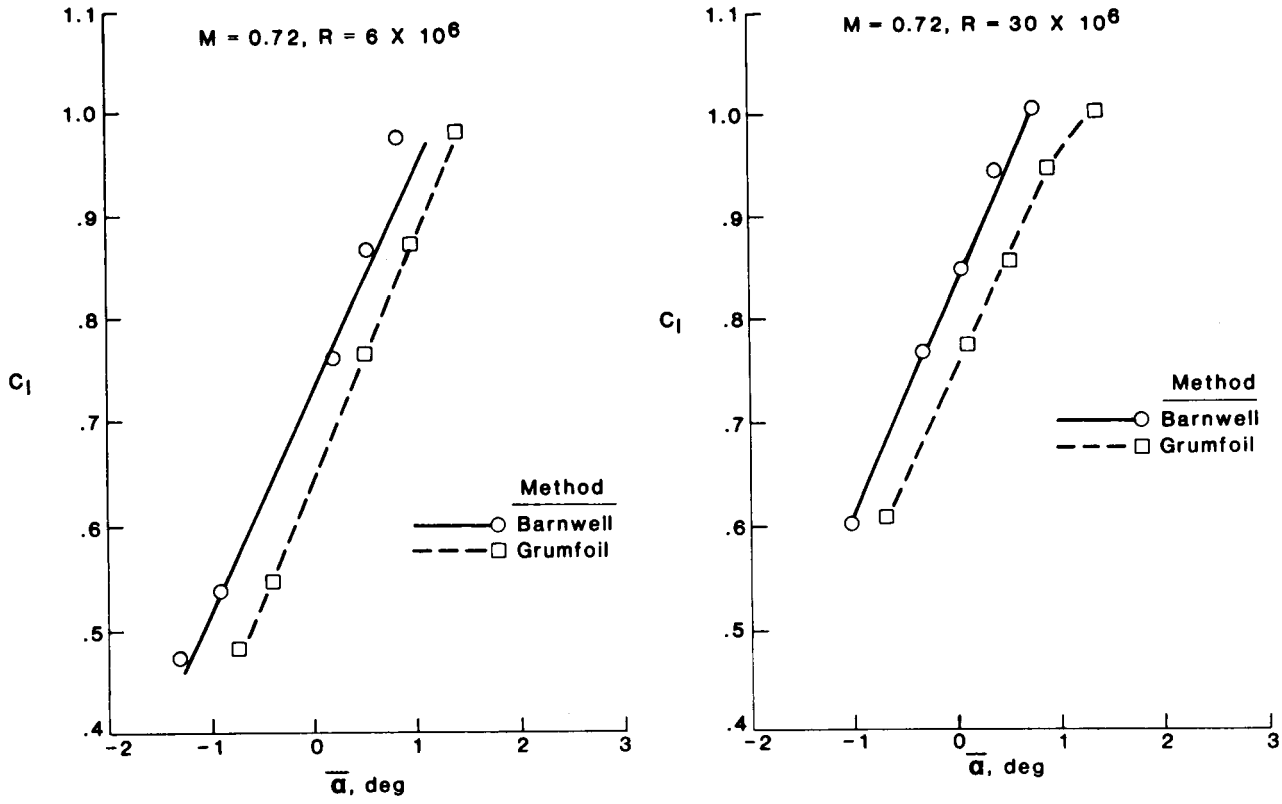

UNSTEADY PRESSURE TEST RESULTS AT A TUNNEL MACH NUMBER OF 0.72 AND AT α = 0.25 DEGREES

$\bar{\alpha}_t = 2.05$ degrees

The effect of Reynolds number and frequency of pitch oscillation on the upper surface unsteady pressure distribution is shown in the next two figures. Results are given in terms of the modulus of the unsteady pressure coefficient normalized by the oscillating pitch angle, α, and the phase angle, ϕ, between the unsteady pressure and the oscillating pitch angle. Results are shown for $\bar{\alpha}_t \approx$ 1 and 2° at R = 6 x 10^6 and 30 x 10^6 for two oscillation frequencies, 5 Hz and 20 Hz at a pitch amplitude of ±0.25°.

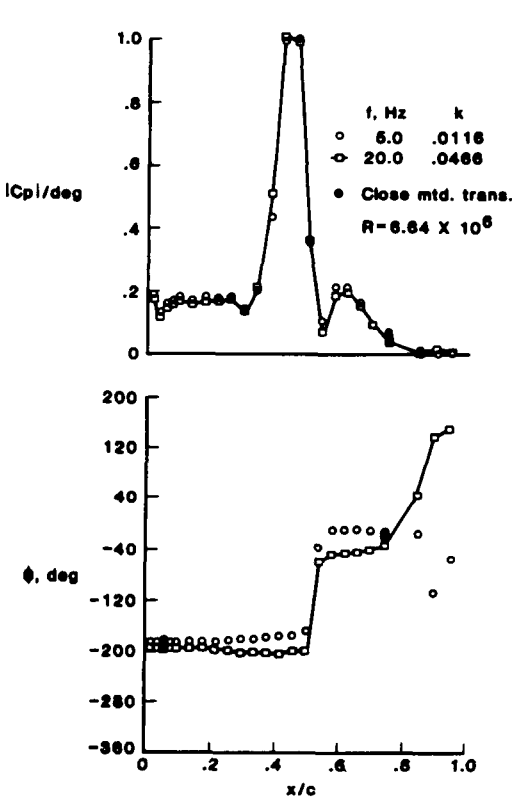

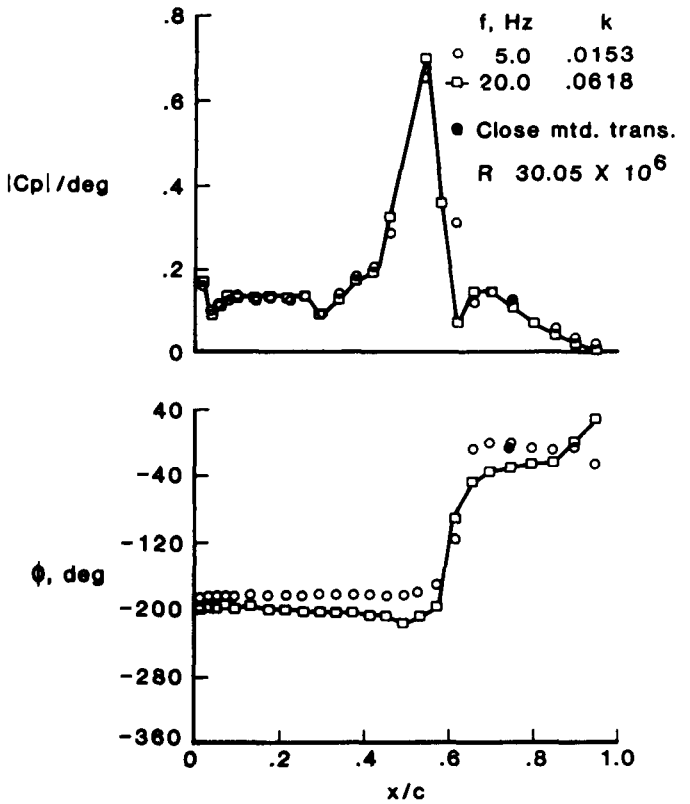

UNSTEADY PRESSURE TEST RESULTS AT A TUNNEL MACH NUMBER OF 0.72 AND AT $\alpha_t = \pm 0.25$ DEGREES

$\bar{\alpha}_t = 1.04$ degrees

The shock wave, identified by the peak in the unsteady pressures, moves aft about 8% to 10% chord as R is increased from 6 x 10^6 to 30 x 10^6 at the same tunnel test angles. The unsteady pressures, at both R, are significantly greater ahead of the shock at $\bar{\alpha}_t$ = 1° than at 2°, but there is no significant difference in the pressure modulus due to the change in frequency from 5 Hz to 20 Hz. For both angles of attack and R the pressures ahead of the shock are approximately 180° out of phase with the wing oscillation. At the shock the phase angle abruptly changes from -180° to 0°. Behind the shock the phase angle is erratic at $\bar{\alpha}_t$ = 1.0° and is more dependent on frequency than at $\bar{\alpha}_t$ = 2.0°.

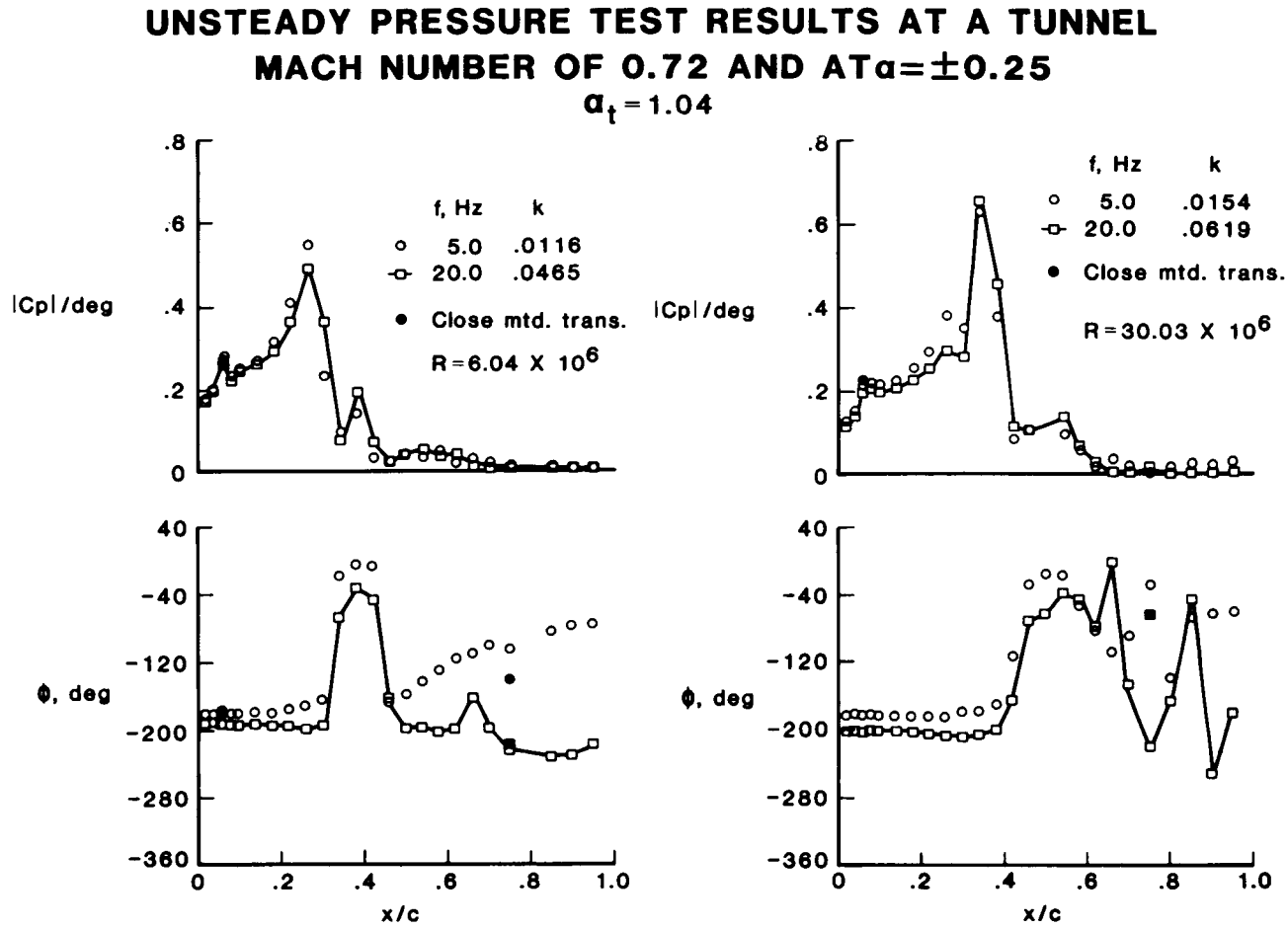

VARIATION OF $|C_p|$/DEGREES AND ϕ WITH PITCH AMPLITUDE AT M = 0.72 AND R = 30 X 10^6 f = 40 HZ

The effect of varying the amplitude of oscillation at M = 0.72 and R = 30 x 10^6 is shown in the next two figures. Upper surface pressure modulus and phase are shown for three pitch amplitudes (0.25, 0.5, 1.0°) at mean angles of 1.0 and 2.0° at f = 40 and 60 Hz. A reduction and broadening of the shock-generated peak amplitude is evident as the pitch amplitude, α, is increased at both frequencies and mean angles.

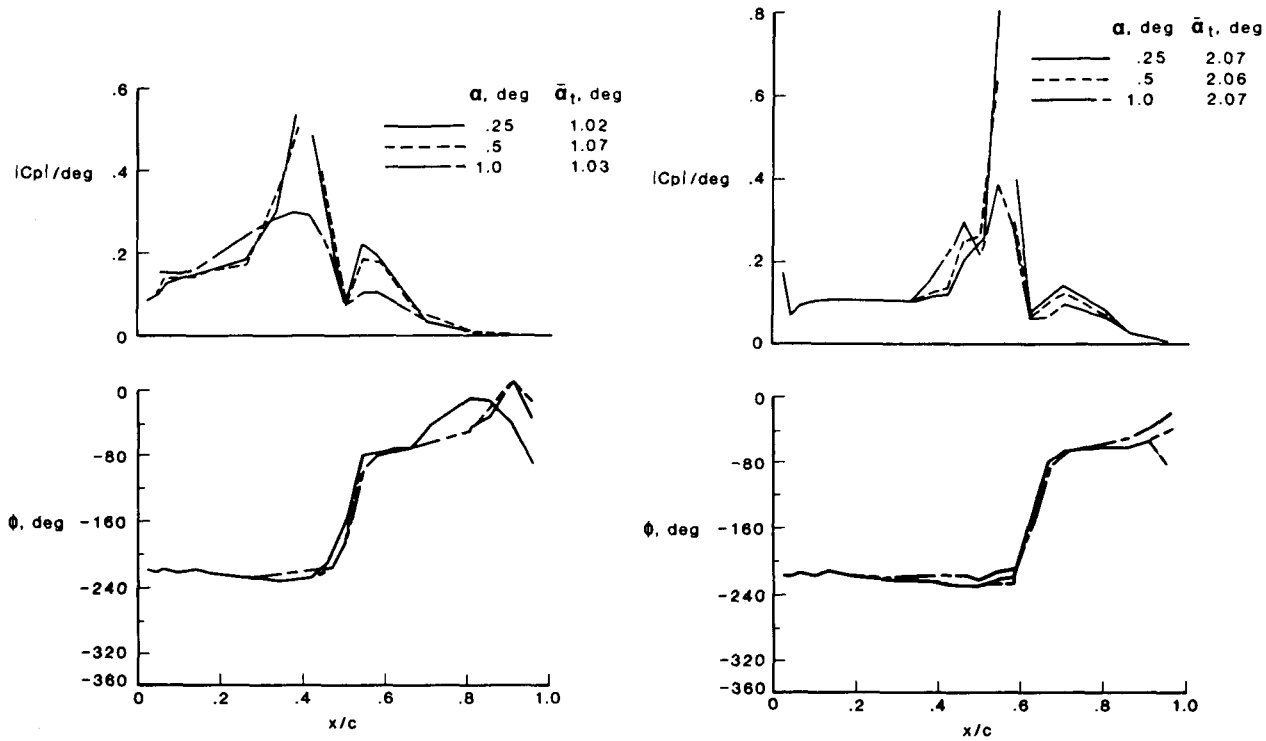

VARIATION OF $|C_p|$/DEGREES AND ϕ WITH PITCH AMPLITUDE AT M = 0.72 AND R = 30 X 10^6 f = 60 HZ

A secondary peak in the modulus of the oscillating pressure is evident immediately behind the shock in this and the other unsteady pressure distribution figures. The amplitude of this second peak is greater at $\bar{\alpha}_t$ = 1.0° than at $\bar{\alpha}_t$ = 2.0°. The phase angle between pressure and wing motion is approximately -180° between the leading edge and immediately behind the shock, at which point there is a sudden decrease to below -80°. There is less deviation in phase for the $\bar{\alpha}_t$ = 2.0° data than for the $\bar{\alpha}_t$ = 1.0° data.

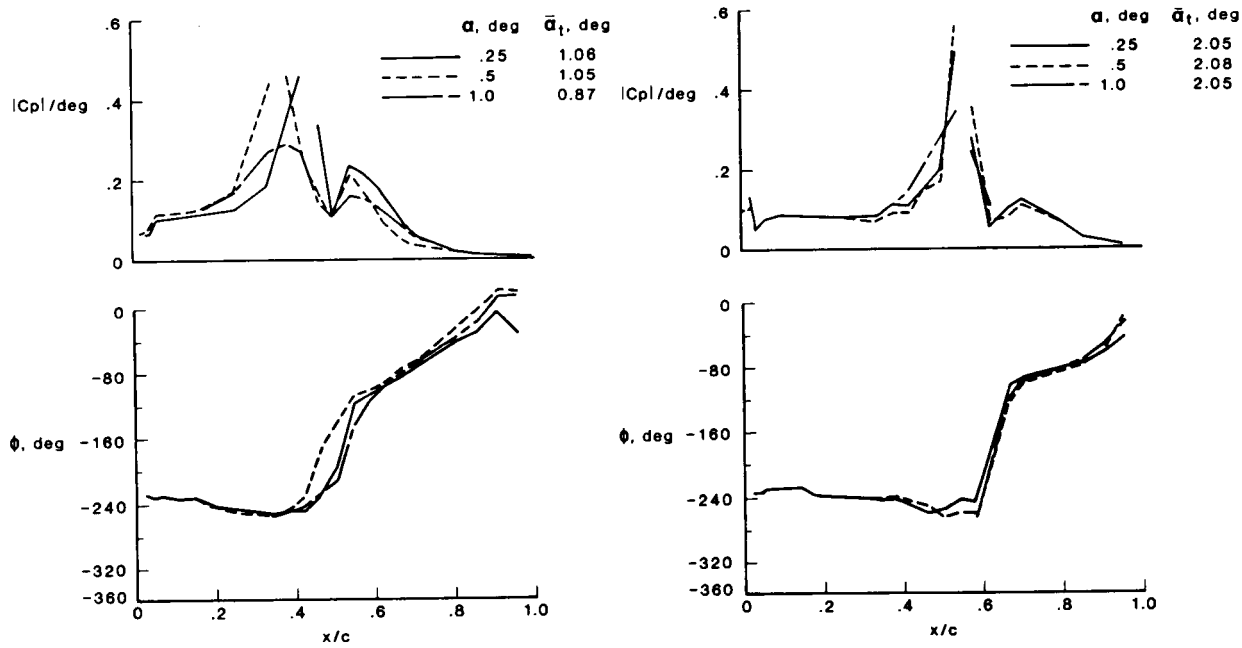

SONIC REGIONS AT M = 0.72 CALCULATED BY GRUMFOIL CODE

The secondary peak in the pressure modulus could be attributed to flow separation and reattachment as discussed in Ref. 9. However, an inviscid calculation using XTRAN2L (Refs. 10,11) computer code predicts this secondary peak in the same relative location. The sonic regions calculated from GRUMFOIL suggests that a more probable reason for the secondary response derives from the supersonic region above the airfoil. At $\bar{\alpha}_t = 1.0^o$ there is a secondary supersonic region behind the shock which is engulfed by the primary supersonic region when the angle of attack is increased to $\bar{\alpha}_t = 2.0^o$. Tijdeman (12) and others have noted that the flow in the supersonic region prior to the formation of a shock is characterized by a substantial increase in unsteady pressure.

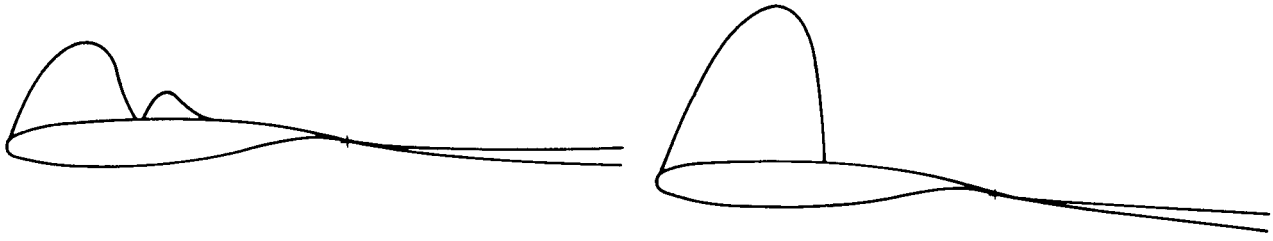

(a) $\bar{\alpha}_t = 1°$ (b) $\bar{\alpha}_t = 2°$

VARIATION OF $|C_p|$/DEGREES AND ϕ WITH FREQUENCY AT M = 0.72 AND R = 30 X 10^6 α = 0.25 DEGREES

The effect of frequency on the modulus and phase of the upper surface unsteady pressures is shown in the next two figures for M = 0.72 and R = 30 x 10^6. The measurements are shown for frequencies of 5, 15, 40, and 60 Hz at mean pitch angles of 1 and 2° and at amplitudes of 0.25 and 0.5°. In general the excursion of the shock is reduced at 60 Hz and again the amplitude of the second peak is reduced for all frequencies as $\bar{\alpha}_t$ is increased from 1.0 to 2.0°.

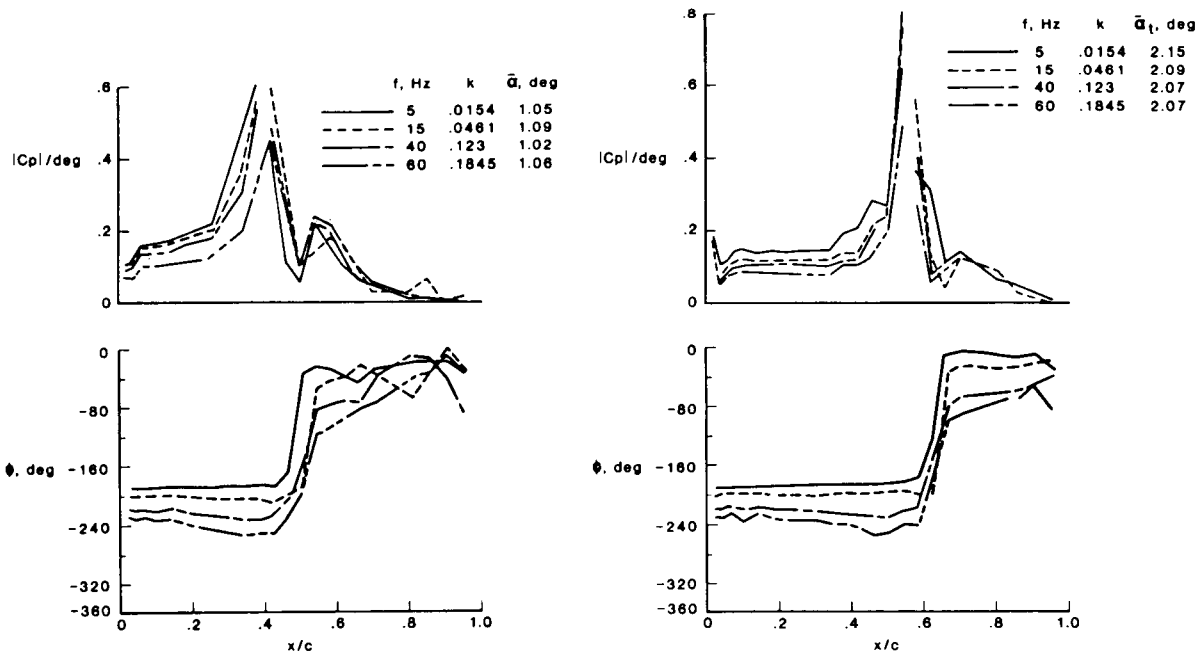

VARIATION OF $|C_p|$/DEGREES AND ϕ WITH FREQUENCY AT M = 0.72 AND R = 30 X 10^6 α = 0.5 DEGREES

The phase angle shows a dependency on frequency in detailed sense having the same overall characteristics as in the previous figures. The phase angle between the pressure and the airfoil motion is approximately - 180° from the leading edge to immediately behind the shock where it increases rapidly to approximately 0°.

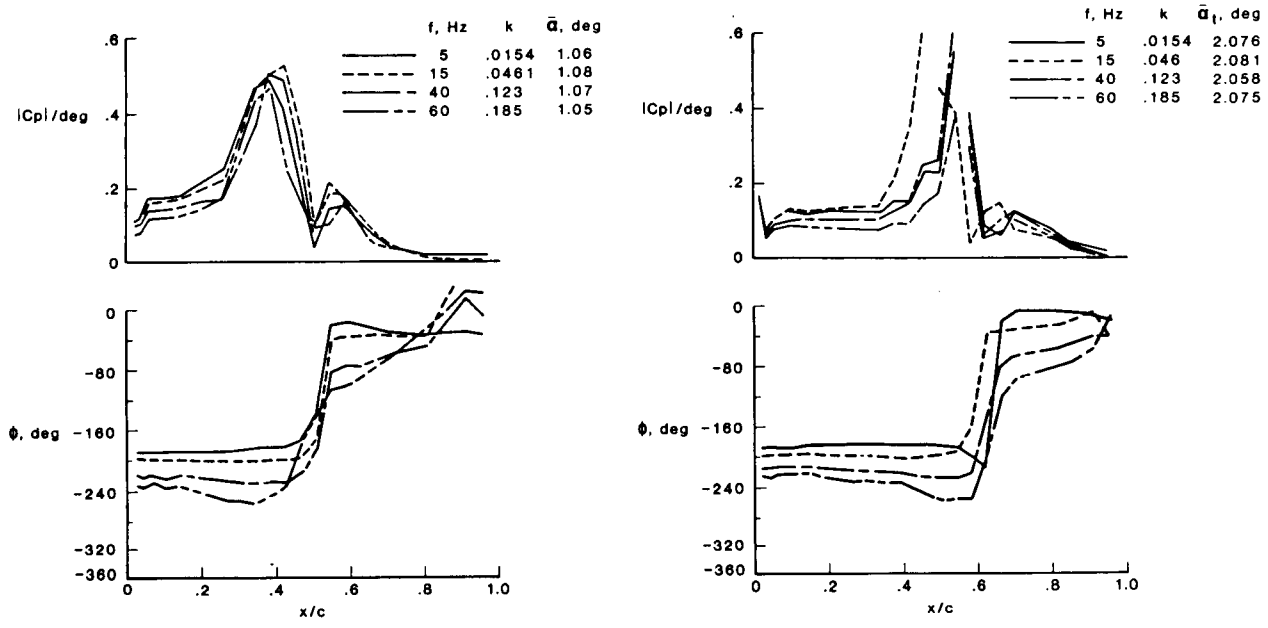

TIME HISTORIES AT FIVE CHORD STATIONS FOR A = 0, M = 0.72, AND R = 35 X 10^6

$\bar{\alpha}_t = 0$ degrees

The pressure transducers used to measure unsteady pressures generated by airfoil pitch oscillation were also used to measure unsteady pressures when the wing was held at a fixed angle of attack. The next two figures show time histories at five chord stations whose locations are shown by solid symbols on the plot of the static pressure distribution, on the right of the figures, for the angles of attack (0 and 2°) being considered. The time histories shown in these figures were all taken at a gain of 10, but the transducer sensitivity, given with each trace, has not been applied to put the data in engineering units.

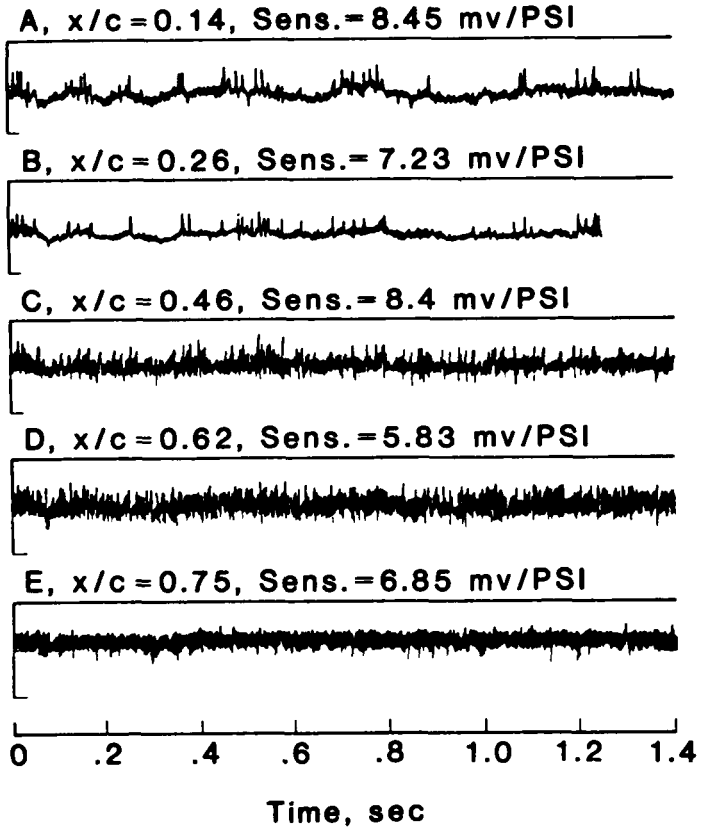

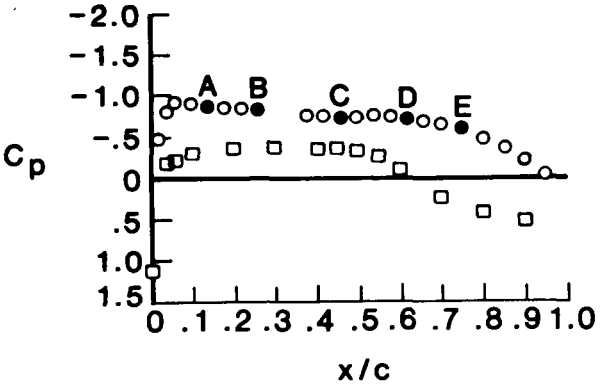

TIME HISTORIES AT FIVE CHORD STATIONS FOR A = 0, M = 0.72, AND R = 35 X 10^6

$\bar{\alpha}_t = 2$ degrees

At $\bar{\alpha}_t = 0^o$ the time histories have the characteristics of a turbulent boundary layer and are in sharp contrast with the time histories of $\bar{\alpha}_t = 2^o$. At $\bar{\alpha}_t$ of 2^o the pressure is quiescent at x/c of 0.14 and 0.28, at x/c of 0.46 the effect of shock movement on the pressure response is observed, which increases at the foot of the shock, x/c = 0.62, where turbulence is also apparent. The observable differences between the flows at the two angles of attack are the more favorable pressure gradient and the presence of a shock wave at $\bar{\alpha}_t = 2^o$. The time histories indicate that laminar flow was present at $\bar{\alpha}_t = 2^o$ and that transition to turbulence was between an x/c of 0.28 and 0.46 corresponding to transition Reynolds numbers between 9.8 x 10^6 and 16.1 x 10^6. The possibility exists that long runs of laminar flow existed intermittently during the tests.

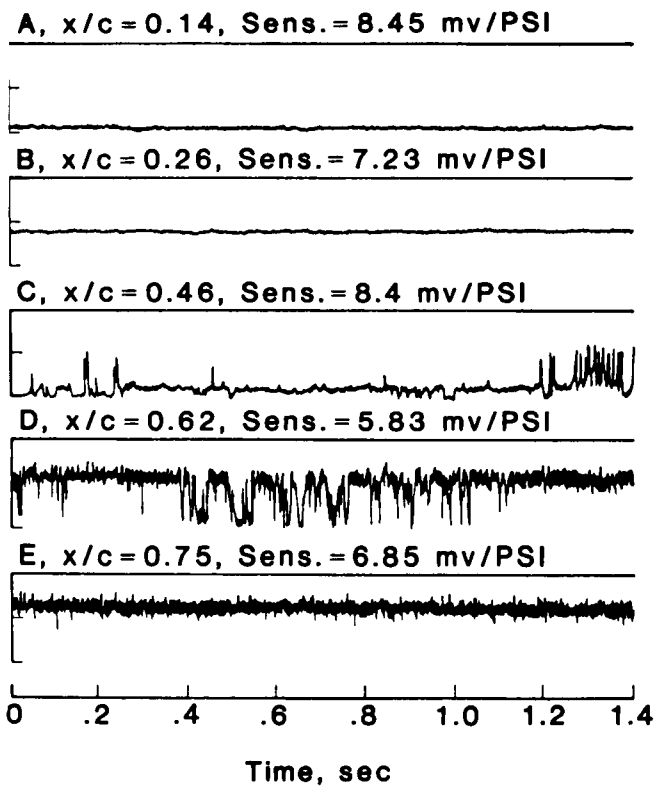

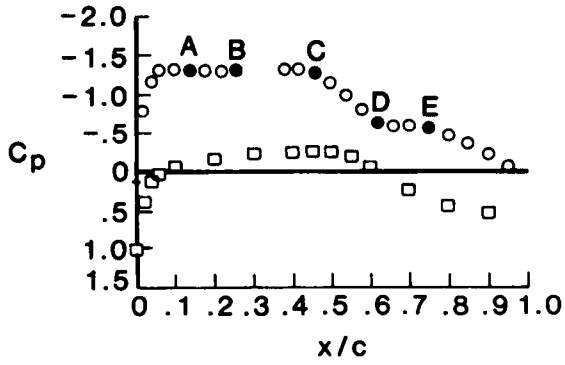

CONCLUSIONS

Steady and unsteady pressures have been measured on a 14 percent supercritical airfoil at transonic Mach numbers at Reynolds numbers from 6×10^6 to 35×10^6. Instrumentation techniques were developed to measure unsteady pressures in a cryogenic tunnel at flight Reynolds numbers. Experimental steady data, corrected for wall effects show very good agreement with calculations from a full potential code with an interacted boundary layer. The steady and unsteady pressures both show a shock position that is dependent on Reynolds number. For a supercritical pressure distribution at a chord Reynolds number of 35×10^6 laminar flow was observed between the leading edge and the shock wave at 45 percent chord.

ACKNOWLEDGMENT

The author wishes to acknowledge the assistance of Clyde Gumbert of the Theoretical Aerodynamics Branch, NASA Langley Research Center, in the Grumfoil calculations.

REFERENCES

[1]Harris, C. D.: "Aerodynamic Characteristics of a 14-Percent Thick NASA Supercritical Airfoil Designed for a Normal-Force Coefficient of 0.7." NASA TM X-72712, July 1975.

[2]Ray, E. J.; Ladson, C. L.; Adcock, J. B.; Lawing, P. L.; and Hall, R. M.: "Review of Design and Operational Characteristics of the 0.3M Transonic Cryogenic Tunnel." NASA TM 80123, 1979.

[3]Ray, E. J.: "A Review of Reynolds Number Studies Conducted in the Langley 0.4M-Transonic Cryogenic Tunnel." AIAA/ASME 3rd Joint Thermophysics, Fluids, Plasma and Heat Transfer Conference, St. Louis, MO, June 7-11, 1982. AIAA Paper 82-0941.

[4]Sewall, W. G.: "The Effects of Sidewall Boundary Layer in Two-Dimensional Subsonic and Transonic Wind Tunnels." AIAA Journal, Vol. 20, No. 9, September 1982, pp. 1253-1256.

[5]Jenkins, R. V.; and Adock, J. B.: "Tables for Correcting Airfoil Data Obtained in the Langley 0.3-Meter Transonic Cryogenic Tunnel for Sidewall Boundary Layer Effects." NASA TM 87723, June 1986.

[6]Barnwell, R. W.: "Design and Performance Evaluation of Slotted Walls for Two-Dimensional Wind Tunnels." NASA TM 78648, February 1978.

[7]Mead, H. R.; and Melnik, R. E.: "GRUMFOIL: A Computer Code for the Viscous Transonic Flow Over Airfoils." NASA CR 3806, October 1985.

[8]Gumbert, C. R.; and Newman, P. A.: "Validation of a Wall Interference Assessment/Correction Procedure for Airfoil Tests in the 0.3M-Transonic Cryogenic Tunnel." AIAA 2nd Applied Aerodynamics Conference, August 21-23, 1984.

[9]Mundell, A. R. G.; and Mabey, D. G.: "Pressure Fluctuations Caused by Transonic Shock/Boundary-Layer Interaction." Aeronautical Journal, August/September 1986.

[10]Whitlow, W., Jr.: "XTRAN2L: A Program for Solving the General Frequency Unsteady Transonic Small Disturbance Equation," NASA TM 85721, November 1983.

[11]Seidel, D. A.; and Batina, J. T.: "User's Manual for XTRAN2L (Version 1.2): A Program for Solving the General-Frequency Unsteady Transonic Small-Disturbance Equation," NASA TM 87737, July 1986.

[12]Tijdeman, H.: "Investigation of the Transonic Flow Around Oscillating Airfoils," NLR TR 77090 U, 1977.